Defeating Jamming Attacks in Downlink Pairwise NOMA Using Relaying

Van-Lan Dao, Svetlana Girs, and Elisabeth Uhlemann
Malardalen University,Västerås, Sweden, {van.lan.dao,svetlana.girs,elisabeth.uhlemann}@mdu.se

***Abstract*—This study explores an incremental relaying strategy in downlink pairwise Non-Orthogonal Multiple Access (NOMA), which involves multiple pairs of nodes near and far from the downlink destinations. The strategy aims to select a near destination node to relay the packet of a far destination node, considering the presence of jamming attacks. To this end, we first derive closed-form expressions for the individual outage probability (IOP) for both near and far destinations in Nakagami-m fading channels. Next, the overall IOP (OIOP) performance is defined as the maximum value among the obtained IOPs, ensuring fairness among the nodes. To optimize the system, simulated annealing algorithms are proposed to determine the best power allocation and the best relay-destination pairing. We can conclude that both the power allocation and the position/selection of the near destination node significantly impact the OIOP for a specific pair. However, in the case of multiple pairs of destinations, a good power allocation alone suffices for each pair, and fixed or even random destination pairing is satisfactory in the considered context.**

***Index Terms*—strong interference, jamming attack, relaying strategy, simulated annealing**

I. Introduction

Multiple access techniques play a crucial role in ensuring the efficient operation of wireless networks across a wide range of applications. Non-Orthogonal Multiple Access (NOMA) is being considered as a promising candidate, particularly for future technologies like 5G and beyond [1], [2] and factory automation [3]–[5]. NOMA-based systems have the potential to provide performance improvements compared to Orthogonal Multiple Access (OMA) systems when appropriately configured [3]. In downlink NOMA, multiple destinations are served simultaneously and share the same time and frequency resources but with different power levels [6]. To separate the signals of each destination at the receiver, a successive interference cancellation (SIC) unit is utilized. In some systems, however, due to the complexity of the SIC unit, it is practical to have a limited number of destinations active simultaneously, such as in pairwise NOMA, which enhances system performance even in the presence of imperfect SIC [7], [8]. To further enhance the performance of NOMA systems, various challenges and open problems need to be addressed [9], [10].

In many practical scenarios, ensuring the smooth operation of applications while preserving the safety of humans necessitates stringent reliability requirements for wireless networks. For instance, in factory automation, the packet error rate must be lower than 10^{-6} [11], [12]. Relaying strategies emerge as promising techniques to meet such demanding reliability requirements in wireless communication [13], [14]. In the context of pairwise NOMA, a near destination must first decode the signal intended for the far destination and subsequently remove it using SIC before decoding its own signal. A protocol, known as incremental relaying [15]–[17], can enhance communication reliability by allowing the near destination to assist in forwarding the far destination's packet in the second phase. The focus of this work lies specifically in investigating this cooperative protocol. In a previous study [15], an energy harvesting-based relaying cooperative NOMA protocol was proposed to maximize system throughput. Both outage probability and throughput were evaluated when the near destination acted as a relayer and energy harvester [16]. Another study [17] proposed a protocol in which the source node could switch between direct NOMA transmission mode and cooperative NOMA transmission mode to minimize the system's outage probability. Additionally, a backscatter cooperation scheme in downlink NOMA was evaluated to highlight the advantages of the proposed approach [18]. In [19], the three user selection schemes are introduced based on the user distances from the source for one pair. The study considered random destination locations and destination pairing schemes for one pair, demonstrating superior performance compared to existing schemes outlined in [20]. However, appropriate power allocation and destination pairing for multiple pairs of destinations still need to be investigated.

Despite the numerous advantages associated with wireless technologies, they are vulnerable to cyber attacks [21]–[23]. Malicious entities, such as jammers, can deliberately generate noise signals to disrupt ongoing wireless transmissions. Consequently, different legitimate nodes may experience varying levels of interference from jamming signals. The National Institute of Standards and Technology (NIST) reported an example of potential attacks through reactive jamming on smart Internet of Things (IoT) systems [24]. Consequently, it becomes crucial to consider the presence of jamming attacks, including any interfering entities, in practical wireless systems. Furthermore, with the significant increase in the number of connected devices, dense deployment and spectrum reuse have become prevalent [25]. As a result, different wireless networks are more likely to interfere with each other, necessitating effective interference management techniques [26]–[28]. In this regard, it is of great practical interest to investigate an incremental relaying scheme and destination pairing in scenar-

The research leading to these results has received funding from the Swedish Foundation for Strategic Research through the Serendipity Project.

ios involving multiple destinations, considering the presence of jamming attacks and/or interfering entities. Thus, the main contributions of this study can be summarized as follows:

- Considering an incremental relaying strategy in the downlink pairwise NOMA system, we derive closed-form expressions for the individual outage probability (IOP) of both the near and far destinations, taking into account the impact of Nakagami-m fading channels.
- To ensure fairness among the near-far destinations, we define the overall IOP (OIOP) as the maximum value obtained from the IOPs. By incorporating both the IOP and OIOP metrics, we can guarantee the stringent requirements for critical services, as enforced by the IOP, while maintaining fairness among the remaining destinations, such as best-effort services, through the OIOP.
- Finally, we use the OIOP to select an appropriate power allocation and near-far pairing for relaying, in the presence of jamming. Our results indicate that both power allocation and the positioning of the near destination have a significant impact on the OIOP for a single pair. However, in the scenario involving multiple pairs of destinations, only power allocation holds a crucial role in enhancing communication reliability. The selection of destination pairing does not significantly influence the OIOP in this context.

The rest of the paper is organized as follows. Section II presents the considered system model. Next, Section III defines and derives a closed-form expression of the IOP for each destination before defining the OIOP. Then, the power allocation and destination pairing optimization are introduced in Section IV. After that, the numerical results are presented in Section V. Finally, Section VI concludes the paper.

II. System Model

We consider a cooperative relaying strategy in downlink pairwise NOMA in the presence of jamming attacks, Fig. 1. In particular, a source node S communicates with a set of far destinations with D_2 and a set of near destinations with D_1. We assume that there are N pairs of destinations (D_1, D_2) one near, one far, and each pair can be served during one slot by using, e.g. Time Division Multiple Access (TDMA). For each pair, in the first phase, the source node sends the superimposed signal to both destinations in downlink pairwise NOMA. At the near destination D_1, D_2's signal is decoded first by treating D_1's signal and the jamming signal as interference. Then, D_2's signal is removed by SIC to decode D_1's signal only considering the jamming signal as interference. At the far destination, D_2's signal is decoded by considering both D_1's signal and the jamming signal as interference. To improve communication reliability for the further destination, D_1 acts as a relayer to forward the received D_2's packet to D_2 using decode-and-forward (DF) in the second phase. There exists a malicious jammer in each phase, in which jamming signals are generated over relevant wireless channels to interrupt ongoing legitimate transmissions. Note that all legitimate nodes are located inside the border and are

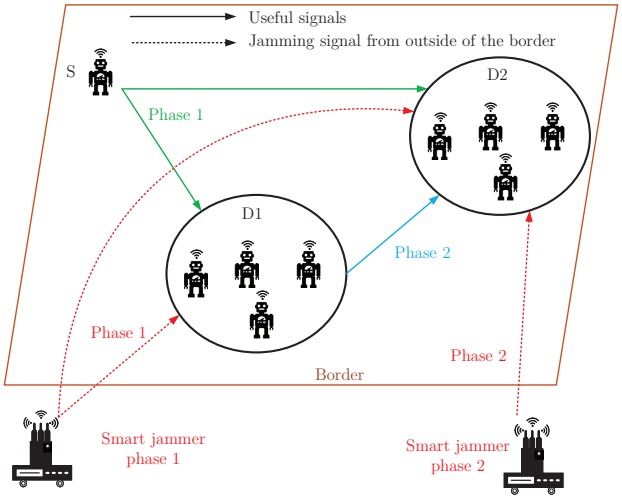

Fig. 1. System model.

protected by fences or walls. In contrast, harmful jammers are only allowed to appear outside of the border, Fig. 1. We assume that all nodes operate in half-duplex mode with a single antenna and all channels follow Nakagami-m fading. In practice, perfect channel state information (CSI) is not available at the transceivers. Therefore, we consider imperfect CSI in this work as

$$\widetilde{g}_x = (\widehat{g}_x + e_x) d_x^{-\frac{\zeta_x}{2}}, \tag{1}$$

where $x = \{SD_1, SD_2, D_1D_2\}$, d_x, ζ_x, $\widehat{g}_x$ and $e_x \sim CN(0, \sigma_x^2)$ are the distance, path-loss exponent, estimated channel coefficient and channel estimation error, respectively.

In the first phase, the received signal-to-interference-plus-noise ratios (SINRs) at the destinations D_2 and D_1 can be represented as

$$\gamma_{D_2} = \frac{(1-\mu_1)\, h_{SD_2}}{\mu_1 h_{SD_2} + h_{J_1.D_2} + \rho_{SD_2}\sigma^2_{SD_2} + 1}, \tag{2}$$

$$\gamma^2_{D_1} = \frac{(1-\mu_1)\, h_{SD_1}}{\mu_1 h_{SD_1} + h_{J_1D_1} + \rho_{SD_1}\sigma^2_{SD_1} + 1}, \tag{3}$$

$$\gamma^1_{D_1} = \frac{\mu_1 h_{SD_1}}{\alpha\,(1-\mu_1)\, h_{SD_1} + h_{J_1D_1} + \rho_{SD_1}\sigma^2_{SD_1} + 1} \tag{4}$$

where $h_{SD_2} = \rho_{SD_2}|\widehat{g}_{SD_2}|^2$, $\rho_{SD_2} = \frac{P_S}{d^{\zeta_{SD_2}}_{SD_2} W\sigma^2_{D_2}}$, $h_{J_1D_2} = \rho_{J_1D_2}|\widetilde{g}_{J_1D_2}|^2$, $\rho_{J_1D_2} = \frac{P_{J_1}}{d^{\zeta_{J_1D_2}}_{J_1D_2} W\sigma^2_{D_2}}$, $h_{SD_1} = \rho_{SD_1}|\widehat{g}_{SD_1}|^2$, $\rho_{SD_1} = \frac{P_S}{d^{\zeta_{SD_1}}_{SD_1} W\sigma^2_{D_1}}$, $h_{J_1D_1} = \rho_{J_1D_1}|\widetilde{g}_{J_1D_1}|^2$, $\rho_{J_1D_1} = \frac{P_{J_1}}{d^{\zeta_{J_1D_1}}_{J_1D_1} W\sigma^2_{D_1}}$. Here, P_S and P_{J_1} are the transmit power of the source node S and the jammer J_1, respectively. Noting that μ_1 is the power allocation factor for the first destination, $0 < \mu_1 < 0.5$. And that channel gains $|.|^2$ are characterized by a Gamma distribution with unit mean and shape m_x and hence $h_x \sim \left(m_x, \frac{\rho_x}{m_x}\right)$.

In the second phase, the received SINR at the destination D_2 is represented as

$$\gamma_{D_2}^{'} = \frac{h_{D_1D_2}}{h_{J_2D_2} + \rho_{D_1D_2}\sigma_{D_1D_2}^2 + 1}, \quad (5)$$

where $h_{D_1D_2} = \rho_{D_1D_2}|\widehat{g}_{D_1D_2}|^2$, $\rho_{D_1D_2} = \frac{P_{D_1}}{d_{D_1D_2}^{\zeta_{D_1D_2}} W\sigma_{D_2}^2}$, $h_{J_2D_2} = \rho_{J_2D_2}|\widetilde{g}_{J_2D_2}|^2$, $\rho_{J_2D_2} = \frac{P_{J_2}}{d_{J_2D_2}^{\zeta_{J_2D_2}} W\sigma_{D_2}^2}$. Here, σ_y^2, $y \in \{D_1, D_2\}$, is the noise spectral density.

III. Outage Probability Analysis

In this section, we first derive closed-form expressions of the IOP for both D_1 and D_2 before defining OIOP for one pair. At the first destination, an outage occurs when *(i)* it fails to correctly decode D_2's signal, and/or *(ii)* even if D_2's signal is decoded and subtracted successfully, D_1's signal still cannot be decoded correctly. In other words, the IOP of the first destination signal is

$$p_1 = 1 - \Pr\left\{\left(\gamma_{D_1}^2 \geq A_2\right) \cap \left(\gamma_{D_1}^1 \geq A_1\right)\right\} \quad (6)$$
$$= 1 - \Pr\left\{h_{SD_1} \geq \max\left(a_1 h_{J_1D_1} + b_1, a_2 h_{J_1D_1} + b_2\right)\right\}, \quad (7)$$

where $a_1 = \frac{A_2}{1-\mu_1(1+A_2)}$, $b_1 = a_0 a_1$, $a_2 = \frac{A_1}{\mu_1(1+\alpha A_1)-A_1\alpha}$, $b_2 = a_0 a_2$, and $a_0 = \rho_{SD_1}\sigma_{SD_1}^2 + 1$. A_1 and A_2 are the thresholds to correctly decode the first and second destination signals, respectively. To ensure that both packets can be decoded correctly at D_1, we found a bound of power allocation factor from (6) as $\frac{A_1\alpha}{1+A_1\alpha} \leq \mu_1 < \min\left\{\frac{1}{1+A_2}, 0.5\right\}$. The closed-form expression of p_1 is derived in the following lemma.

Lemma 1. *Given that* $h_{SD_1} \sim G\left(m_{SD_1}, \frac{\rho_{SD_1}}{m_{SD_1}}\right)$ *and* $h_{J_1D_1} \sim G\left(m_{J_1D_1}, \frac{\rho_{J_1D_1}}{m_{J_1D_1}}\right)$*, the closed-form expression of* p_1 *can be obtained as follows:*

$$p_1 = \begin{cases} 1 - I_1 & \mu_1 \geq \frac{A_1(1+A_2\alpha)}{A_2(1+A_1\alpha)+A_1(1+A_2)} \\ 1 - I_2 & \mu_1 < \frac{A_1(1+A_2\alpha)}{A_2(1+A_1\alpha)+A_1(1+A_2)} \end{cases}, \quad (8)$$

where

$$I_j = \frac{\left(m_{J_1D_1}\rho_{J_1D_1}^{-1}\right)^{m_{J_1D_1}} e^{-m_{SD_1}\rho_{SD_1}^{-1}b_j}}{\Gamma(m_{J_1D_1})} \sum_{k=0}^{m_{SD_1}-1} \times \frac{\left(m_{SD_1}\rho_{SD_1}^{-1}b_j\right)^k}{k!} \sum_{l=0}^{k} \binom{k}{l} \left(\frac{a_j}{b_j}\right)^l \frac{\Gamma\left(m_{J_1D_1}+l\right)}{\rho_j^{m_{J_1D_1}+l}},$$

where $j \in \{1, 2\}$, $\rho_j = m_{J_1D_1}\rho_{J_1D_1}^{-1} + m_{SD_1}\rho_{SD_1}^{-1}a_j$.

Proof. Applying [8, Theorem 1], this lemma is proved. ■

At the far destination D_2, an outage occurs if the following conditions occur: *(i)* D_2's signal cannot be decoded successfully at D_2 by considering D_1's signal and the jamming signal as interference in the first phase and *(ii)* D_2's signal cannot be decoded correctly at D_1 in the first phase and/or D_2 cannot decode correctly D_2's signal in the second phase. Accordingly, the IOP for the second destination's signal is expressed as follows:

$$p_2 = 1 - \Pr\left\{\left(\gamma_{D_2} \geq A_2\right) \cup \left[\left(\gamma_{D_1}^2 \geq A_2\right) \cap \left(\gamma_{D_2}^{'} \geq A_2\right)\right]\right\},$$
$$= 1 - I_3 - I_1 I_4 + I_3 I_1 I_4, \quad (9)$$

where

$$I_3 = \Pr\left\{\gamma_{D_2} \geq A_2\right\} = \Pr\left\{h_{SD_2} \geq a_3 h_{J_1D_2} + b_3\right\}, \quad (10)$$
$$I_4 = \Pr\left\{\gamma_{D_2}^{'} \geq A_2\right\} = \Pr\left\{h_{D_1D_2} \geq a_4 h_{J_2D_2} + b_4\right\}, \quad (11)$$

where $a_3 = \frac{A_2}{1-\mu_1(1+A_2)}$, $b_3 = b_0 a_3$, $b_0 = \rho_{SD_2}\sigma_{SD_2}^2 + 1$, $a_4 = A_2$, $b_4 = c_0 a_4$, and $c_0 = \rho_{D_1D_2}\sigma_{D_1D_2}^2 + 1$. The closed-form expression of p_2 is derived in the following lemma.

Lemma 2. *Given that* $h_{SD_2} \sim G\left(m_{SD_2}, \frac{\rho_{SD_2}}{m_{SD_2}}\right)$, $h_{J_1D_2} \sim G\left(m_{J_1D_2}, \frac{\rho_{J_1D_2}}{m_{J_1D_2}}\right)$*, and* $h_{J_2D_2} \sim G\left(m_{J_2D_2}, \frac{\rho_{J_2D_2}}{m_{J_2D_2}}\right)$*, the closed-form expression of* I_j, $j \in \{3, 4\}$*, can be obtained as follows:*

$$I_j = \frac{\left(m_X\rho_X^{-1}\right)^{m_X} e^{-m_Y\rho_Y^{-1}b_j}}{\Gamma(m_X)} \sum_{k=0}^{m_Y-1} \times \frac{\left(m_Y\rho_Y^{-1}b_j\right)^k}{k!} \sum_{l=0}^{k} \binom{k}{l} \left(\frac{a_j}{b_j}\right)^l \frac{\Gamma\left(m_X+l\right)}{\rho_j^{m_X+l}},$$

where $X \in \{J_1D_2, J_2D_2\}$, $Y \in \{SD_2, D_1D_2\}$, *and* $\rho_j = m_X\rho_X^{-1} + m_Y\rho_Y^{-1}a_j$.

Proof. Applying [8, Theorem 1], this lemma is obtained. ■

The fairness condition among the destinations is also an important requirement as shown in [29]. To ensure this requirement, we define a reliability metric namely OIOP as follows:

$$O_i = \max\{p_1, p_2\}_i, i \in \{1, .., N\}. \quad (12)$$

The benefit of this metric is that we can guarantee strict requirements for critical services in terms of IOP as constraints, while for the rest of the services, best efforts can be guaranteed with the fairness condition using the OIOP when we formulate the problem for various applications.

IV. Optimizing Power Allocation and Destination Pairing

When all destinations have the same priority and requirements on, e.g. the communication reliability level, the main goal of the legitimate wireless communication system is to maximize communication reliability in terms of minimizing the maximum OIOP among all pairs by changing the destination pairing and power allocation factor for each pair during the first phase. Accordingly, the main problem can be formulated as follows:

$$(\text{P1}): \underset{\mu_{1.i}, \text{destination pairing}}{\text{minimize}} \quad \max\{O_i\} \quad (13a)$$
$$\text{s.t.} \quad \frac{A_1\alpha}{1+A_1\alpha} \leq \mu_{1.i} < \min\left\{\frac{1}{1+A_2}, 0.5\right\} \quad (13b)$$

where $\mu_{1.i}$ is the power allocation factor for the i^{th} pair.

TABLE I
THE FUNCTIONS FINDING THE OPTIMAL POWER ALLOCATION FACTOR FOR EACH PAIR AND THE BEST DESTINATION PAIRING.

Name	*PA_one_pair*	*DP_N_pairs*
Configurations	T_1, ϵ_1, N_1	T_2, ϵ_2, N_2
Input paramters	$d_{x.i}$, $\zeta_{x.i}$, $\sigma^2_{x.i}$, $\sigma^2_{y.i}$, $m_{x.i}$, P_S, $P_{D_{1.i}}$, P_{J_1}, P_{J_2}, A_1, A_2, W	d_x, ζ_x, σ^2_x, σ^2_y, m_x, P_S, P_{D_1}, P_{J_1}, P_{J_2}, A_1, A_2, W
Output paramters	$\mu_{1.i.opt}$	The best destination pairing
Cost function	O_i in (12)	$\max\{O_i\}$ in (15a)
Solution S	$\mu_{1.i}$	Destination pairing

To solve the problem (P1), we separate it into two sub-problems as follows: *(i)* For each pair of the two destinations, we find $\mu_{1.i}$ to minimize O_i in (12) as presented in (14a), and *(ii)* We select the best destination pairing for all destinations of D_1 and D_2 to minimize the maximum OIOP among all pairs as in (15a).

$$\text{(P1A)}: \underset{\mu_{1.i}}{\text{minimize}} \quad O_i \tag{14a}$$

$$\text{s.t.} \quad \frac{A_1\alpha}{1+A_1\alpha} \leq \mu_{1.i} < \min\left\{\frac{1}{1+A_2}, 0.5\right\} \tag{14b}$$

$$\text{(P1B)}: \underset{\text{destination pairing}}{\text{minimize}} \quad \max\{O_i\}, \forall \in \{1,2,...,N\} \tag{15a}$$

To address the problems in (14a) and (15a), we adopt the Simulated Annealing (SA) algorithm according to **Algorithm 1** in [30] and as described in table I. The *PA_one_pair* and *DP_N_pairs* functions find the best power allocation for one pair and the best destination pairing for the multiple pairs scenario, respectively. T_1 and T_2 are the algorithm temperatures and ϵ_1 and ϵ_2 are the factors to update the temperatures in the next iteration. N_1 and N_2 are the numbers of iterations.

V. RESULTS

In this section, we present numerical results for the IOP and OIOP of the considered system. The following system parameters are used: $W = 1$ Hz, $P_S = 10$ W, $P_{D_1} = 1$ W, $m_{SD_1} = m_{SD_2} = m_{D_1D_2} = 2$, $m_{J_1D_1} = m_{J_1D_2} = m_{J_2D_2} = 1$, $\zeta_{SD_1} = \zeta_{SD_2} = \zeta_{D_1D_2} = 2$, $\zeta_{J_1D_1} = \zeta_{J_1D_2} = \zeta_{J_2D_2} = 3$, $A_1 = A_2 = 2^{\frac{R_{th}}{W}} - 1$ where R_{th} is the target rate, $\alpha = 1e-4$, $\sigma^2_{SD_1} = \sigma^2_{SD_2} = \sigma^2_{D_1D_2} = 1e-4$, and $\sigma^2_{D_1} = \sigma^2_{D_2} = 10^{-10}$ W/Hz [8], [31]. The border is defined as $(y = -10, -\infty < x < \infty)$. For the SAs, all configuration parameters are selected manually, $T_1 = T_2 = 0.01$, $\epsilon_1 = \epsilon_2 = 0.9$, and $N_1 = N_2 = 1000$. To validate the correctness of the analysis in section III, computer simulations are conducted using MATLAB. For each considered IOP, we generate 10^6 samples of the channel gains following a Gamma distribution and then check the outage conditions for each destination. The simulation results of the IOPs are then obtained by taking the average of all outage events across 10^6 samples.

Fig. 2 demonstrates the effect of the power allocation factor μ_1 on the IOP for each destination in three cases as follows: $(x_S, y_S) = (0,0)$, $(x_{D_2}, y_{D_2}) = (100,-10)$, $(x_{J_1}, y_{J_1}) = (50,-30)$, $(x_{J_2}, y_{J_2}) = (100,-15)$, $P_{J_1} = P_{J_2} = 10$ W, C1: $(x_{D_1}, y_{D_1}) = (25,10)$, C2: $(x_{D_1}, y_{D_1}) = (50,10)$, C3: $(x_{D_1}, y_{D_1}) = (75,10)$. Note that different positions of D_2 are presented in Fig. 3. It can be seen from the figure that the analytical and simulation results match very well. Moreover, the IOP of D_1 decreases significantly when the power allocation factor increases and D_1 is located closer to the source node S. This is because the path loss impact is compensated by an increase of transmit power from the source node and a smaller distance between the source node and destination D_1. However, the IOP of the second destination goes up slightly, even supported by one transmission more from the first destination. The reason is that the transmit power for the second destination reduces when the power allocation factor increases. Especially, the effect of a jamming attack from J_2 is very strong due to the fact that both D_2 and J_2 stay very close to the border.

In Fig. 3, the OIOPs for the three aforementioned cases are presented for different positions of D_2. We can see that we can

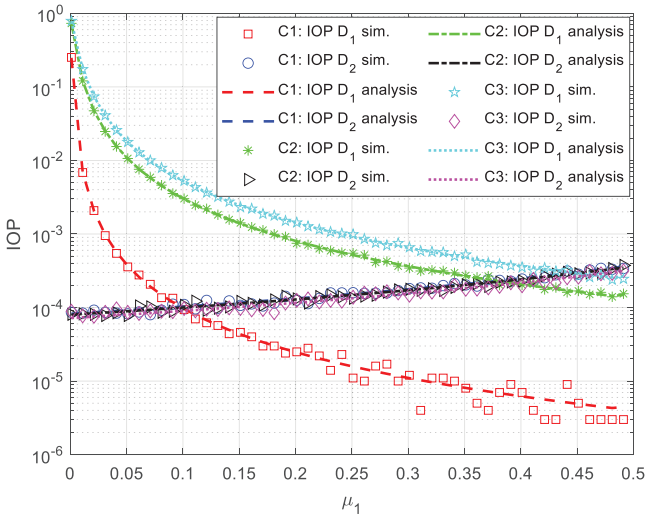

Fig. 2. The IOPs versus power allocation factor.

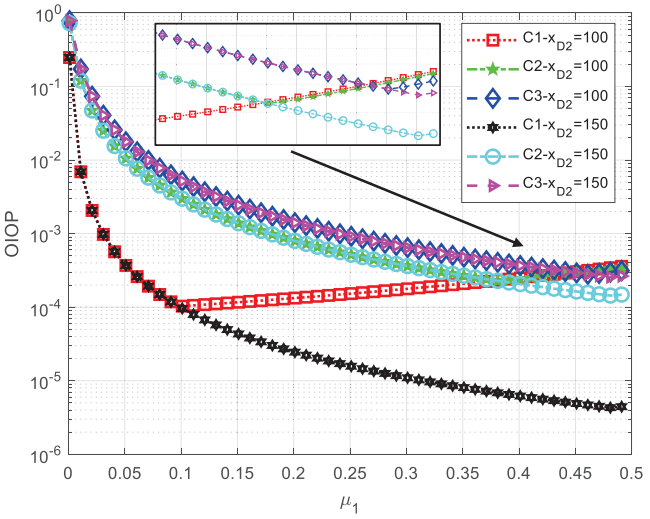

Fig. 3. The OIOP versus power allocation factor.

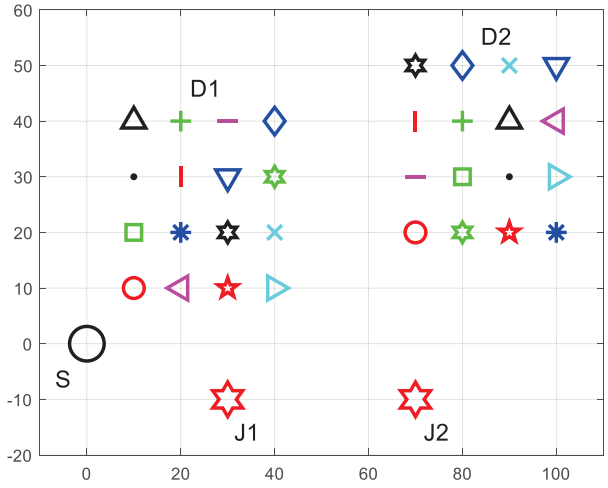

Fig. 4. The destination pairing when $(x_{J_1}, y_{J_1}) = (30, -10)$ and $(x_{J_2}, y_{J_2}) = (70, -10)$.

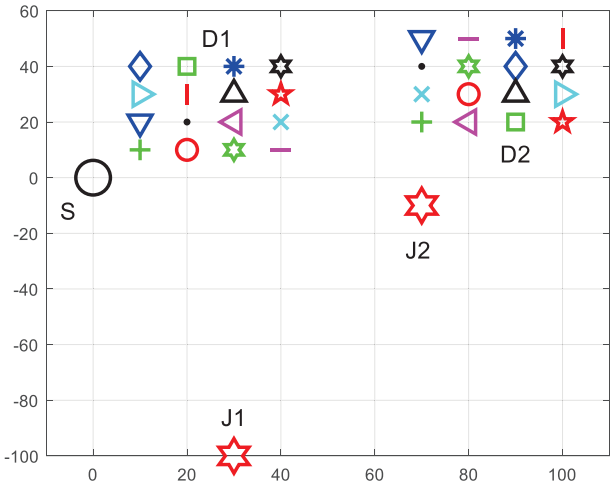

Fig. 6. The destination pairing when $(x_{J_1}, y_{J_1}) = (30, -100)$ and $(x_{J_2}, y_{J_2}) = (70, -10)$.

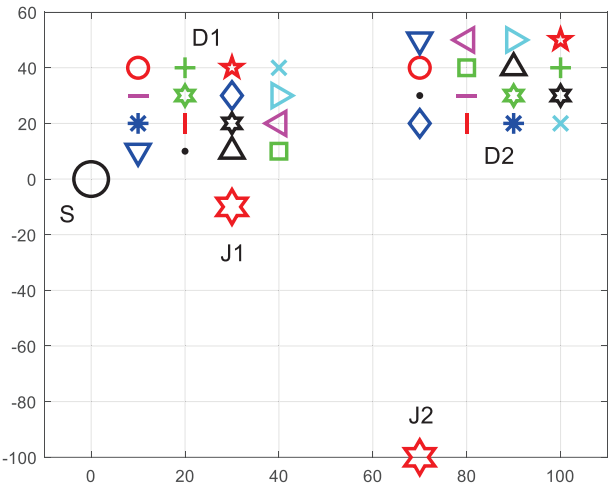

Fig. 5. The destination pairing when $(x_{J_1}, y_{J_1}) = (30, -10)$ and $(x_{J_2}, y_{J_2}) = (70, -100)$.

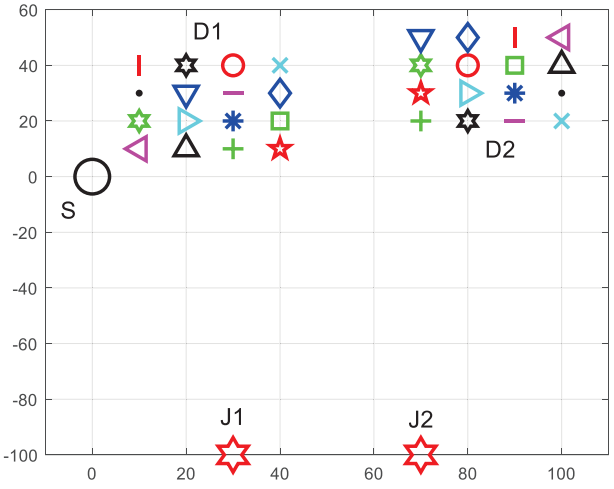

Fig. 7. The destination pairing when $(x_{J_1}, y_{J_1}) = (30, -100)$ and $(x_{J_2}, y_{J_2}) = (70, -100)$.

find the optimal power allocation factor to minimize the OIOP for different cases. Moreover, these power allocation factors are affected dramatically by the first destination's position when $x_{D_2} = 100$. When $x_{D_2} = 150$ and $x_{D_1} = 25$, the OIOP decreases significantly due to less interference from both jammers at D_2 and a smaller path-loss effect at D_1. As a result, finding both the best power allocation factor and D_1's position is very important to enhance the communication reliability of one pair of legitimate users.

By using the SA algorithms in table I for various cases of jammers' positions in Figs. 4-7 with $P_{J_1} = P_{J_2} = 5$W, we can find the best destination pairing. We also found that J_1's position affects significantly the OIOP, while the effect of J_2's position is negligible, Fig. 8. Moreover, the fluctuation of the OIOP around the converged value is negligible, Fig. 8. From the figures Figs. 4-7, the destination pairing does not follow any rule. Consequently, destination pairing is not important in the multiple pairs of destinations scenario, while power allocation is crucial. To verify this conclusion, we also compare the optimal $\max\{O_i\}$ using the SA algorithms and random destination pairing (average of 1000 times) in table II.

Based on the obtained results, we make two important conclusions: *(i)* both power allocation and D_1's position significantly affect the OIOP, and *(ii)* only power allocation is important in the multiple destinations scenario.

VI. Conclusion

In this paper, a cooperative relaying strategy in downlink pairwise NOMA with multiple destinations scenario is considered. Closed-form expressions of the IOPs for both

TABLE II
THE MAXIMUM OIOP AMONG ALL PAIRS FOR FIGS. 4-7.

$\max\{O_i\}$	Fig. 4	Fig. 5	Fig. 6	Fig. 7
Optimal	4.91e-04	4.91e-04	4.13e-08	4.13e-08
Random (mean)	4.91e-04	4.91e-04	4.13e-08	4.13e-08
Random (max)	4.93e-04	4.93e-04	4.17e-08	4.15e-08

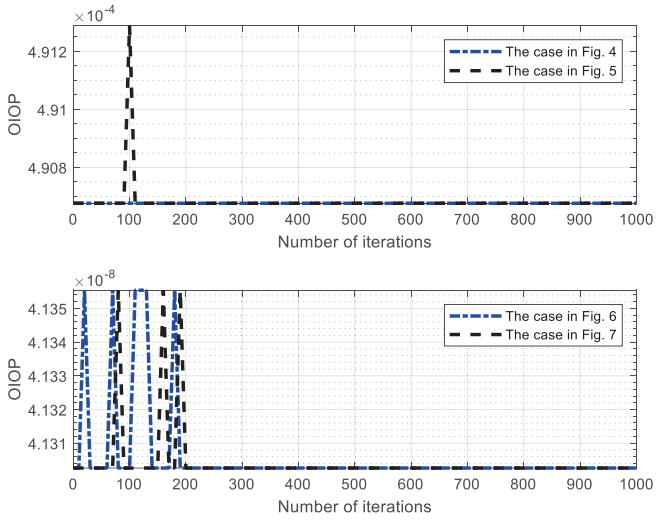

Fig. 8. The OIOP versus a number of iterations using the proposed SAs for the cases in Figs. 4-7.

destinations are obtained in the presence of jamming for Nakagami-m fading channels. We define the OIOP based on the obtained IOPs to guarantee a fairness condition. By using SA, we found that the power allocation and the position of the first destination are very important for one pair. However, destination pairing is not needed in the scenario with multiple pairs of destinations. Therefore, only optimal power allocation is needed in the case of multiple destinations, and using fixed destination pairing would cause no performance reduction.

REFERENCES

[1] I. Budhiraja, N. Kumar, S. Tyagi, S. Tanwar, Z. Han, M. J. Piran, and D. Y. Suh, "A systematic review on NOMA variants for 5G and beyond," *IEEE Access*, vol. 9, pp. 85 573–85 644, 2021.

[2] Y. Liu, S. Zhang, X. Mu, Z. Ding, R. Schober, N. Al-Dhahir, E. Hossain, and X. Shen, "Evolution of NOMA toward next generation multiple access (NGMA) for 6G," *IEEE JSAC*, vol. 40, no. 4, pp. 1037–1071, 2022.

[3] J. Montalban, E. Iradier, P. Angueira, O. Seijo, and I. Val, "NOMA-based 802.11n for industrial automation," *IEEE Access*, vol. 8, pp. 168 546–168 557, 2020.

[4] E. Iradier, L. Fanari, I. Bilbao, J. Montalban, P. Angueira, O. Seijo, and I. Val, "Analysis of NOMA-based retransmission schemes for factory automation applications," *IEEE Access*, vol. 9, pp. 29 541–29 554, 2021.

[5] Y. Wang, M. Zheng, and H. Yu, "NODR: An NOMA-based retransmission scheme for URLLC in industrial wireless networks," *IEEE Sensors Journal*, vol. 22, no. 20, pp. 20 073–20 084, 2022.

[6] A. Benjebbour, K. Saito, A. Li, Y. Kishiyama, and T. Nakamura, "Non-orthogonal multiple access (NOMA): concept and design," *Signal processing for 5G: Algorithms and implementations*, pp. 143–168, 2016.

[7] L. Dai, B. Wang, Y. Yuan, S. Han, C. I, and Z. Wang, "Non-orthogonal multiple access for 5G: solutions, challenges, opportunities, and future research trends," *IEEE Commun. Mag.*, vol. 53, no. 9, pp. 74–81, Sep. 2015.

[8] V.-L. Dao, L.-N. Hoang, S. Girs, and E. Uhlemann, "Outage performance of pairwise NOMA allowing a dynamic decoding order and optimal pairs of power levels," *IEEE OJCOMS*, vol. 1, pp. 1886–1906, 2020.

[9] A. F. M. S. Shah, A. N. Qasim, M. A. Karabulut, H. Ilhan, and M. B. Islam, "Survey and performance evaluation of multiple access schemes for next-generation wireless communication systems," *IEEE Access*, vol. 9, pp. 113 428–113 442, 2021.

[10] Y. Mao, O. Dizdar, B. Clerckx, R. Schober, P. Popovski, and H. V. Poor, "Rate-splitting multiple access: Fundamentals, survey, and future research trends," *IEEE COMST*, vol. 24, no. 4, pp. 2073–2126, 2022.

[11] Z. Ma, M. Xiao, Y. Xiao, Z. Pang, H. V. Poor, and B. Vucetic, "High-reliability and low-latency wireless communication for internet of things: Challenges, fundamentals, and enabling technologies," *IEEE Internet of Things Journal*, vol. 6, no. 5, pp. 7946–7970, 2019.

[12] P. Sanz, I. Val, A. Urkidi, P. Angueira, and J. Montalban, "Safety related systems design methodology for wireless time-varying channels," in *IEEE WFCS*, 2021, pp. 123–130.

[13] S. Diggavi, N. Al-Dhahir, A. Stamoulis, and A. Calderbank, "Great expectations: the value of spatial diversity in wireless networks," *Proceedings of the IEEE*, vol. 92, no. 2, pp. 219–270, 2004.

[14] Z. Ding, H. Dai, and H. V. Poor, "Relay selection for cooperative NOMA," *IEEE WCL*, vol. 5, no. 4, pp. 416–419, 2016.

[15] K. Reshma and A. V. Babu, "Throughput analysis of energy harvesting enabled incremental relaying NOMA system," *IEEE COMML*, vol. 24, no. 7, pp. 1419–1423, 2020.

[16] Y. Liu, Y. Ye, H. Ding, F. Gao, and H. Yang, "Outage performance analysis for SWIPT-based incremental cooperative NOMA networks with non-linear harvester," *IEEE COMML*, vol. 24, no. 2, pp. 287–291, 2020.

[17] G. Li, D. Mishra, and H. Jiang, "Cooperative NOMA with incremental relaying: Performance analysis and optimization," *IEEE Transactions on Vehicular Technology*, vol. 67, no. 11, pp. 11 291–11 295, 2018.

[18] W. Chen, H. Ding, S. Wang, D. B. da Costa, F. Gong, and P. H. Juliano Nardelli, "Backscatter cooperation in NOMA communications systems," *IEEE TWC*, vol. 20, no. 6, pp. 3458–3474, 2021.

[19] Y. Liu, Z. Ding, M. Elkashlan, and H. V. Poor, "Cooperative non-orthogonal multiple access with simultaneous wireless information and power transfer," *IEEE Journal on Selected Areas in Communications*, vol. 34, no. 4, pp. 938–953, 2016.

[20] Y. Ren, B. Ren, X. Zhang, T. Lv, W. Ni, and G. Lu, "Impartial cooperation in SWIPT-assisted NOMA systems with random user distribution," *IEEE Transactions on Vehicular Technology*, pp. 1–16, 2023.

[21] F. Pan, Z. Pang, M. Luvisotto, M. Xiao, and H. Wen, "Physical-layer security for industrial wireless control systems: Basics and future directions," *IEEE Industrial Electronics Magazine*, vol. 12, no. 4, pp. 18–27, 2018.

[22] H. Pirayesh and H. Zeng, "Jamming attacks and anti-jamming strategies in wireless networks: A comprehensive survey," *IEEE COMST*, vol. 24, no. 2, pp. 767–809, 2022.

[23] P. Angueira, I. Val, J. Montalban, O. Seijo, E. Iradier, P. S. Fontaneda, L. Fanari, and A. Arriola, "A survey of physical layer techniques for secure wireless communications in industry," *IEEE COMST*, vol. 24, no. 2, pp. 810–838, 2022.

[24] V.-L. Dao, L.-N. Hoang, S. Girs, and E. Uhlemann, "Defeating jamming using outage performance aware joint power allocation and access point placement in uplink pairwise NOMA," *IEEE OJCOMS*, vol. 2, pp. 1957–1979, 2021.

[25] Cisco. (2020, March) Cisco annual internet report (2018–2023). [Online]. Available: https://www.cisco.com/c/en/us/solutions/collateral/executive-perspectives/annual-internet-report/white-paper-c11-741490.html

[26] K. Yang, "Interference management in LTE wireless networks [industry perspectives]," *IEEE Wireless Commun.*, vol. 19, no. 3, pp. 8–9, 2012.

[27] A. Willig, K. Matheus, and A. Wolisz, "Wireless technology in industrial networks," *Proc. of the IEEE*, vol. 93, no. 6, pp. 1130–1151, 2005.

[28] S. Yan, X. Cao, Z. Liu, and X. Liu, "Interference management in 6G space and terrestrial integrated networks: Challenges and approaches," *Intell. and Converged Netw.*, vol. 1, no. 3, pp. 271–280, 2020.

[29] S. Timotheou and I. Krikidis, "Fairness for non-orthogonal multiple access in 5G systems," *IEEE Signal Processing Letters*, vol. 22, no. 10, pp. 1647–1651, 2015.

[30] V.-L. Dao, L.-N. Hoang, S. Girs, and E. Uhlemann, "Defeating jamming using outage performance aware joint power allocation and access point placement in uplink pairwise NOMA," *IEEE OJCOMS*, vol. 2, pp. 1957–1979, 2021.

[31] H. Tabassum, M. S. Ali, E. Hossain, M. J. Hossain, and D. I. Kim, "Uplink vs. downlink NOMA in cellular networks: Challenges and research directions," in *Proc. IEEE VTC*, Sydney, NSW, Australia, 2017, pp. 1–7.